Final Report

InCo: Inline Cofactor Monitoring

Inline quantification of NADH und NADPH under process conditions

Aneta Pashkova, Susanne Leuchs, Jonathan Bloh,

Lasse Greiner und Jens Schrader

Mai 2017

Inhalt

1. Allgemeine Angaben

1.1. DFG-Geschäftszeichen

GR 2282/1-1

1.2. Antragsteller

Prof. Dr. Lasse Greiner (z.Z. Hochschule Mannheim, Institut für Biochemie)
Projektleiter: Prof. Dr. Jens Schrader(DECHEMA Forschungsinstitut SbR)

1.3. Institut/Lehrstuhl

Prof. Dr. Lasse Greiner
Hochschule Mannheim / Institut für Biochemie
Paul-Wittsack-Str. 10, D-68163 Mannheim
Tel.: +49 6212926872
l.greiner@hs-mannheim.de

Projektleiter: Prof. Dr. Jens Schrader
DECHEMA Forschungsinstitut / AG Industrielle Biotechnologie
Theodor-Heuss-Allee 25, D-60486 Frankfurt am Main
Tel: +49 697564422
schrader@dechema.de

1.4. Thema des Projekts

Inline quantification of NADH und NADPH under process conditions (Inline Quantifizierung von NADH und NADPH unter Prozessbedingungen)

1.5. Berichtszeitraum, Förderungszeitraum insgesamt

01.01.2012 – 31.01.2017

1.6. Liste der wichtigsten Publikationen aus diesem Projekt

a) Susanne Leuchs, Shukrallah Na'amnieh and Lasse Greiner “Enantioselective reduction of sparingly water-soluble ketones: continuous process and recycle of the aqueous buffer system”, Green Chem. 15 (2013) 167-176, doi:10.1039/C2GC36558H.

   Susanne Leuchs, Joana Lima-Ramos, Lasse Greiner, Naweed Al-Haque, Pär Tufvesson and John M. Woodley, Reaction Engineering of Biocatalytic Enantioselective Reduction: A Case Study for Aliphatic Ketones, Org. Process Res. Dev. 17/8 (2013) 1027–1035, doi: 10.1021/op400117t

b) Susanne Leuchs „Continuous Enzymatic Synthesis of Enantiopure Aliphatic (R)-2-Alcohols” DECHEMA Forschungsinstitut Forschungsberichte Nr. 2, Shaker Verlag ISBN 978-3-8440-2249-0 (2013), Dissertation

   Susanne Bohl, Ionische Flüssigkeiten bei der enzymatischen Ketoreduktion in wässrig-organisch en Zweiphasensystem (2014) DECHEMA-Forschungsinstitut, Bachelorarbeit.

2. Arbeits- und Ergebnisbericht

2.1. Ausgangsfragen und Zielsetzung des Projektes

The redox cofactors nicotinamide adenine dinucleotide (NAD) and nicotinamide adenine dinucleotide phosphate (NADP) are ubiquitous as redox mediators for in vivo and in vitro applications. Their technical importance has grown over the last decades as more and more redox biotransformations have been developed as an asset to highly selective reductions and oxidations catalysed by enzymes dependent on them (Enzyme class 1, oxidoreductases). Even though NAD^+ and NADH are nowadays marketed as a food supplement and relatively cheap [1], $NADP^+$ remains expensive even after a price drop [2]. This is very often considered to be prohibitive for economically viable processes. And despite their discovery already decades ago and their technical relevance today, there is a lack of recent quantitative studies covering the knowledge gap between predictions of cofactor concentrations based on initial rate measurements and their actual application in processes. Furthermore, particularly the reduced cofactors (NADH and NADPH), possess restricted stability which varies over several orders of magnitude with relatively small shifts in reaction conditions. Therefore, the optimisation of any enzymatic process would require quantitative knowledge of the concentrations of the cofactors involved and understanding of their degradation and stabilization mechanisms.

The main goal of the project is the inline quantification of cofactors under process conditions by means of fluorescence spectrometry (FS) allowing monitoring at µmol L^{-1} concentrations, typical for their application. Five main project objectives (O1 – O5) have been summarised in the proposal:

O1: Establish and validate FS for the analysis of reduced cofactors.
O2: Establish inline monitoring under steady-state conditions in batch and continuous mode.
O3: Investigate enzymatic systems based on initial rate measurements.
O4: Characterise coupled systems of increasing complexity under reaction conditions.
O5: Obtain quantitative data and mechanistic understanding on cofactor stability under reaction conditions.

2.2. Entwicklung der durchgeführten Arbeiten

During the course of the project the targeted objectives have been addressed as follows:
O1: fulfilled. Both microplate FS measurements as well as fiber optical FS measurements of NADPH concentrations have been established and validated in the range of 1 µmol L^{-1} to 100 µmol L^{-1}. Stable calibration factors have been obtained for routine use under process conditions (see Chapter 2.3.1).

O2: fulfilled. Inline monitoring of NADPH concentrations has been established for both batch and continuous operation (see Chapter 2.3.5). Integration of the FS-probe in a batch reactor has been demonstrated. For the continuous type of measurements the FS-probe has been integrated in a flow cell module at the reactor outlet. Experimental difficulties and practical considerations did not allow the integration of the probe directly inside the enzyme membrane reactor (EMR). However, as the concentrations of substances in a CSTR type reactor are the same inside the reactor as they are in the outlet, measurement in the outlet is sufficient.

O3: fulfilled. Based on initial rate measurements the reduction of 2-octanone to *(R)*-2-octanol catalysed by an alcohol dehydrogenase from *Lactobacillus brevis* (*Lb*ADH) has been thoroughly investigated. A monophasic approach was developed (aqueous buffer phase with addition of an ionic liquid as solubiliser) as well as enzyme coupled cofactor regeneration with glucose dehydrogenase from *Bacillus spec* (GDH) and glucose as hydride donor (cosubstrate) was implemented (see Chapter 2.3.4.). For both batch and continuous synthesis a mathematical model with Michaelis-Menten type kinetics has been developed and implemented for process optimisation (see Chapter 2.3.3).

O4: fulfilled. Online monitoring of cofactor concentrations has been demonstrated for the monophasic system in batch and continuous mode. Comparison with model predictions as well as with offline measurements has been used as a tool for process optimisation (see Chapter 2.3.5.).

O5: fulfilled. NADPH stability and factors influencing its degradation has been thoroughly investigated. The effects of pH, temperature, light intensity, presence and concentration of salts or oxygen have been summarised further in the report (see Chapter 2.3.2).

2.3. Darstellung der erreichten Ergebnisse und Diskussion

2.3.1. Implementation of measurement techniques

Three different instruments were available for cofactor concentration measurement:

- UV/VIS-multiplate reader (Powerwave HT, BioTek), absorbance mode only, Gen 5 Software.
- UV/VIS-multiplate fluorescence reader (Synergy Mx, BioTek), excitation and emission mode, Gen 5 Software.
- Fluorescence probe (Hellma®, Jena/Müllheim Germany) coupled to a LED-light source with a wavelength of 365 nm and a CCD UV-NIR 200-980 nm detector, nominal power < 500 mW (tec5, Oberursel/Ts Germany), MultiSpec Pro Software (Figure 2.3.1-1).

Both multiplate readers have been used for initial rate measurements, and NADPH/$NADP^+$ half-life time determination. The FS-probe has been used to measure the stability of the cofactors at different light intensities (Figure 2.3.2-2). It has also been integrated in the continuous set-up for the online analysis of the cofactor.

All instruments have been calibrated for cofactor concentrations of up to 100 µmol L^{-1}. The FS-Multiplate reader and the FS-probe have also been calibrated at the same conditions and with the same NADPH standard solutions, in order to use the FS-Multiplate reader as off-line analysis tool to verify the response of the FS-probe during the online measurements (Figure 2.3.5-8).

Because of the instability of NADPH under UV irradiation most of the measurements with the FS-probe were performed at only 5% lamp intensity, which significantly lowers the accuracy and detection limit of the technique. However, at a later project stage, the use of a shutter has been implemented allowing working at 100% lamp intensity while avoiding unnecessary sample irradiation between measurement points. Thus the lower limit of detection was improved from 10 µmol·L^{-1} to 1 µmol·L^{-1} NADPH (Figure 2.3.1-2).

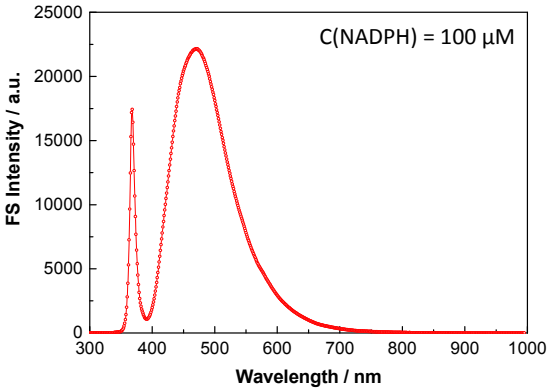

Figure 2.3.1-1: Fluorescence spectrum of NADPH obtained with the FS-probe at 100% lamp intensity and 365 nm excitation wavelength.

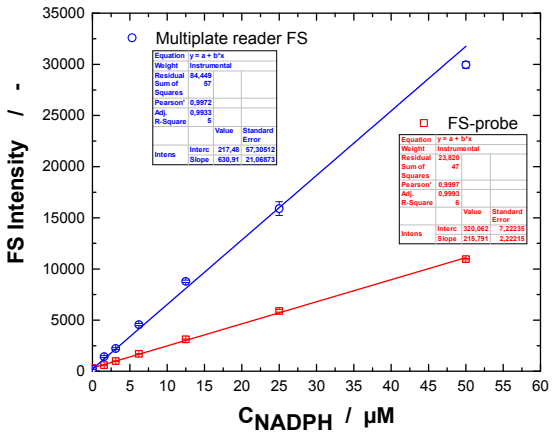

Figure 2.3.1-2: Simultaneous calibration of the FS-Probe (squares) and multi plate reader fluorescence (circles) for the range up to 50 µM NADPH. Excitation wavelength – 360 nm.

2.3.2. NADPH degradation and stability

For the enantioselective enzymatic reduction of 2-octanone to (*R*)-2-octanol (Figure 2.3.3-1) an enzyme coupled cofactor regeneration system based on glucose and GDH (glucose dehydrogenase) has been chosen and implemented. Nevertheless, due to degradation, not all of the cofactor could be recycled. As quantitative results for cofactor stability in literature are contradictory and only available for relatively high concentrations, the half-live times of NADPH and $NADP^+$ were investigated for conditions resembling the process as close as possible and for the main influences of pH, light intensity, presence of oxygen, temperature as well as presence and concentration of salts (including ionic liquids and buffers). It turned out, that depending on experimental conditions, $NADP^+$ is at least ten to thousand times more stable than its reduced form NADPH. For this reason, the focus was brought to the stability of NADPH.

Influence of pH

The dependency of the cofactor half-life time on the pH of the solution was investigated in the range of pH = 6-8 with initial cofactor concentrations from 1.6 µmol·L^{-1} to 100 µmol·L^{-1} (Figure 2.3.2-1). As

expected [3], the stability of NADPH increases with increasing pH. Interestingly, the half-life time seems to be dependent on the initial cofactor concentration at pH greater than 7.5. Normally, a (pseudo)-first order exponential decay is assumed for cofactor degradation. Our data do not support this over the full pH and concentration range. Unfortunately, literature data do not cover the concentration range below 50 µmol·L^{-1}, which is of relevance for our work, as in cofactor regeneration the steady-state concentrations of NADPH are deliberately low. The behaviour that the half-life time increases with increasing cofactor concentration suggests mixed zero and first order kinetics with likely more than one degradation pathway.

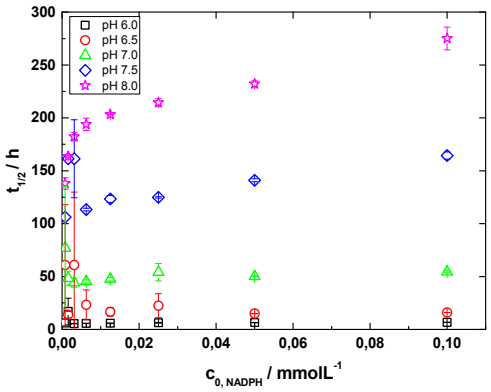

Figure 2.3.2-1: Half-life times of NADPH as a function of pH and initial concentration: $c_{ADA\text{-}buffer}$ = 100 mmol·L^{-1}, c_{MgCl2} = 20 mmol·L^{-1}, T = 25°C.

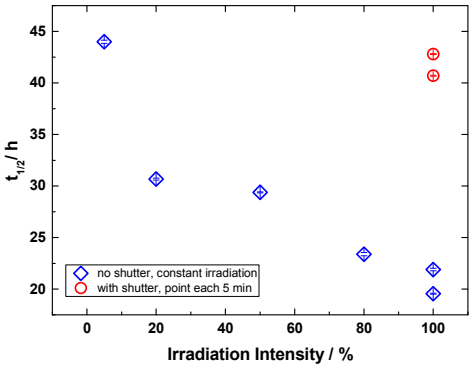

Figure 2.3.2-2: Stability of NADPH as a function of the relative LED irradiation intensity at 365 nm: pH 7.0, c_{NADPH} = 50 µmol·L^{-1}, $c_{ADA\text{-}buffer}$ = 100 mmol·L^{-1}, c_{MgCl2} = 20 mmol·L^{-1}, T = 25°C

Influence of light intensity

These experiments were performed with the FS-probe in a 30 ml brown glass cell to minimize the impact of environmental light sources. The half-life time of NADPH as a function of the LED intensity between 5 and 100% of the maximum output is represented in Figure 2.3.2-2. With the initial version of the FS set-up and the software, the LED light source was always switched on during the whole measurement and thus the NADPH/buffer solution was under constant irradiation (diamonds in Figure 2.3.2-2). In this case a clear dependency is observed: by increasing light intensity, the NADPH half-life time decreased from 44 h to ca. 20 h. At a later project stage a possibility to modulate the light source and work with a shutter was implemented, so that the sample was irradiated only for a short period of 120 ms during each measurement. This leads to a significant increase in NADPH half life time at 100% intensity (circles in Figure 2.3.2-2) and at the same time an improvement of the lower limit of detection by an order of magnitude from 10 µmol·L^{-1} to 1 µmol·L^{-1} NADPH. The dependency on sampling frequency was investigated as well (Table 2.3.2-1) and it was found that decreasing the sampling interval from once per 5 minutes did not further increase the cofactor stability.

Sampling interval	N_2 saturation	O_2 saturation
1 s (constant irradiation)	16.4	14.4
300 s (each 5 min)	23.9	23.9
3600 s (each 1 h)	23.7	23.1

Table 2.3.2-1: NADPH half life time (h) measured with the FS-probe set-up at 100% lamp intensity, 120 ms irradiation and different sampling intervals. pH 7.0, c_{NADPH} = 50 µmol·L^{-1}, $c_{ADA\text{-}buffer}$ = 100 mmol·L^{-1}, c_{MgCl2} = 20 mmol·L^{-1}, T = 25°C.

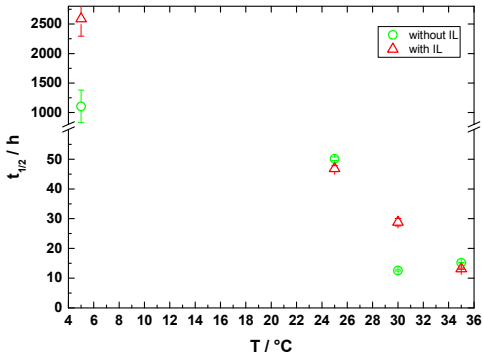

Figure 2.3.2-3: Stability of NADPH as a function of temperature without IL (circles) and with TEGO IL K5 (triangles): pH 7.0, c_{IL} = 100 g·L^{-1}; c_{NADPH} = 50 µmol·L^{-1}, $c_{ADA\text{-}buffer}$ = 100 (150 with IL) mmol·L^{-1}, c_{MgCl2} = 20 mmol·L^{-1}.

Influence of oxygen in the system

Suspecting a role of oxygen presence for accelerated NADPH degradation, experiments for NADPH stability were performed with the FS-probe in a different set-up with 100 ml total volume and a possibility for gas saturation (either N_2 or O_2) of the NADPH/buffer solutions as well as with the use of a shutter to modulate the LED source. The results indicate that the presence of O_2 in the system only has an effect on degradation in combination with constant irradiation (Table 2.3.2-1) and it is not necessary to keep the reaction solution under inert conditions when the shutter is used. Likely, the photoinduced degradation mechanism is accelerated in the presence of oxygen. As no significant difference between 300 s and 3600 s sampling interval has been observed, 300 s (each 5 min) has been chosen as optimal for the online measurements with the continuous system.

Influence of temperature

The stability of NADPH was investigated with and without addition of a solubiliser (ionic liquid) at different temperatures (Figure 2.3.2-3) as well as for different ADA-Buffer concentrations (Figure 2.3.2-4). As expected, the half-life time of NADPH decreases dramatically at higher temperatures and is higher at low temperatures. A general influence of the IL (TEGO IL K5) cannot be deduced. The stability of NADPH was also determined in the pH range from 6.0 - 7.5 with and without 100 $g \cdot L^{-1}$ IL as a function of initial NADPH concentration at various temperatures. A common trend which was observed for nearly all experiments is, that at high pH (pH 7.0 and 7.5) the half-life is increasing with increasing initial cofactor concentration, at low pH (pH 6.0 and 6.5), the half-life is more or less independent on the initial concentration (see also Figure 2.3.2-1). Thus, the assumption of a first order degradation mechanism only holds true for low pH, and is apparently different at high pH.

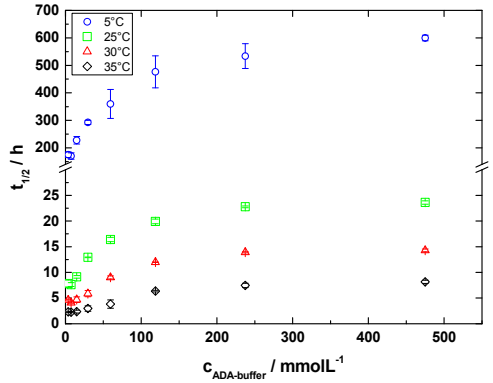

Figure 2.3.2-4: Stability of NADPH in presence of different ADA-buffer concentrations at different temperatures: pH 7.0, c_{MgCl2} = 20 mmol·L^{-1}.

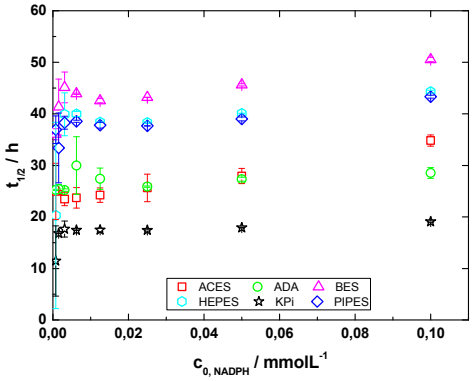

Figure 2.3.2-5: Stability of NADPH in presence of different buffer-salts at pH 7.0, $c_{all\text{-}buffers}$ = 100 mmol·L^{-1}, c_{MgCl2} = 20 mmol·L^{-1}, T = 25°C.

Influence of presence and concentration of salts

Stability of NADPH was investigated in six different buffers (with pK_A close to 7): ACES, ADA, BES, HEPES, KPi (as a reference), and PIPES. The results are summarised in Figure 2.3.2-5. The most commonly used KPi-buffer resulted in the lowest half-lives measured. Better for the NADPH stability were ADA, ACES, HEPES, PIPES, and BES in ascending order. The low stability of NADPH in ADA-buffer might be caused by the acetate moieties in this molecule. Although, ADA-buffer is not the best buffer for NADPH stability, all further experiments were carried out in this one, as a compromise for relatively low price and positive effect on enzyme stability.

Furthermore, experiments concerning the stability of NADPH as a function of ADA-buffer concentration were carried out at 25°C as well as at 5°C, 30°C and 35°C (Figure 2.3.2-4). A hyperbolic increase of half-life with the ADA concentration was observed, optimal stability was achieved by using 120 mmol·L^{-1} ADA-buffer or higher.

A stabilisation effect by Mg^{2+}-ions was found as well, in line with literature data. Therefore, the half-life of NADPH was investigated at $MgCl_2$ concentrations between 1.5 and 190 mmol·L^{-1} (Figure 2.3.2-6). In the range between 1.5 and 95 mmol·L^{-1} no stabilisation effect by $MgCl_2$ was observed, but at 190 mmol·L^{-1} $MgCl_2$, a strong increase in half-life from 20 h to 120 h was observed.

The presence of other salts like ionic liquids can also affect the stability of NADPH. In contrast to the findings reported in literature, in our study strong stabilising effects of the IL were only observed when high concentrations were applied. Furthermore, at 35°C, no stabilising effect of the IL was observed (Figure

2.3.2-7). The applied IL is a surfactant/tenside. The behaviour of such substances in combination with others is complex and might be the reason for the observed inconclusive results.

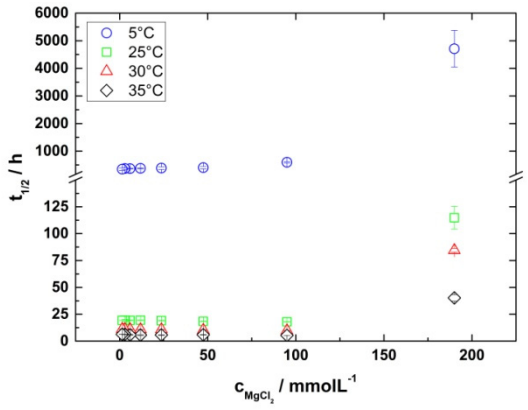

Figure 2.3.2-6: Stability of NADPH in presence of different $MgCl_2$ concentrations at pH 7.0; c_{NADPH} = 50 µmol L^{-1}, $c_{ADA\text{-}buffer}$ = 100 mmol·L^{-1}.

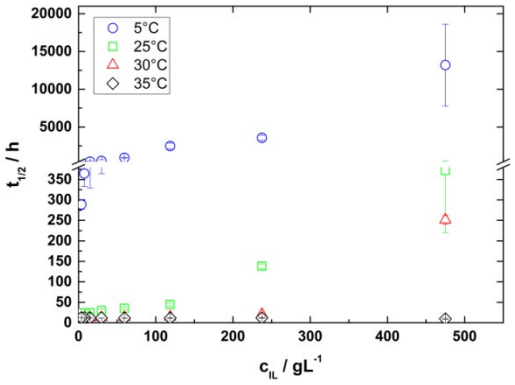

Figure 2.3.2-7: Stability of NADPH in presence of different TEGO IL K5 concentrations at pH 7.0; c_{NADPH} = 50 µmol L^{-1}, $c_{ADA\text{-}buffer}$ = 100 mmol·L^{-1}, c_{MgCl2} = 20 mmol·L^{-1}.

2.3.3. Initial rate measurements and modelling of reaction kinetics

Based on initial rate measurements the reduction of 2-octanone to 2-octanol catalysed by *Lb*ADH has been thoroughly investigated. A monophasic approach was developed as well as enzyme coupled cofactor regeneration with GDH and glucose as cosubstrate was implemented (Figure 2.3.3-1, as well as Chapter 2.3.4). With the addition of an ionic liquid (TEGO IL K5) as solubiliser the amount of the hardly water soluble substrate in the aqueous phase was significantly increased (from 5 up to 94 mmol L^{-1} 2-octanone at 100 g L^{-1} TEGO IL).

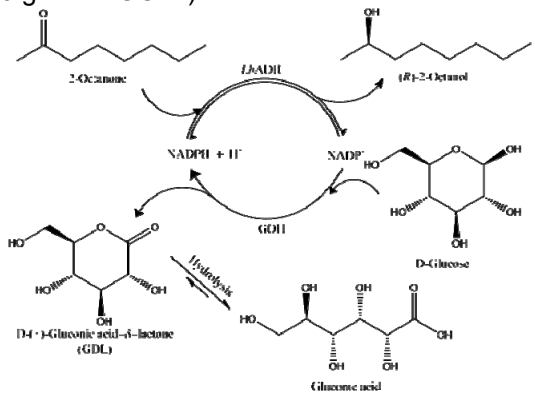

Figure 2.3.3-1: Reaction system for the enantioselective reduction of 2-octanone with enzyme coupled cofactor regeneration.

Reaction	M	B	R
Enzyme	LbADH	LbADH	GDH
2-8ON	S1	P1	-.
2-8OL	P1	S1	-
NADPH	S2	P2	P2
NADP+	P2	S2	S2
Glucose	I1	I1	S1
GDL	I2	I2	P1

Table 2.3.3-1: Interaction matrix. M = main reaction (reduction of 2-octanone to (R)-2-octanol); B = back reaction (oxidation of (R)-2-octanol to 2-octanone); R = cofactor-regeneration.

The main reaction (M) of LbADH (Figure 2.3.3-2), its back reaction (B) and the cofactor-regeneration reaction with GDH (R) were investigated independently for all substrates at IL concentrations of 0, 100, and 200 g L^{-1} based on initial rate measurements performed with the UV/VIS-multiplate fluorescence reader (Synergy Mx, BioTek). The respective interaction matrix is given in Table 2.3.3-1.
It turned out that inhibition of the *Lb*ADH-catalysed reaction by glucose or GDL was relevant. Uncompetitive inhibition was identified and was assumed to be applicable for all *Lb*ADH catalysed experiments. The parameters of a modified Michaelis-Menten model (
Eq. 2.3.3-1) were then estimated using OriginLab 8G.

Eq. 2.3.3-1:
$$v = v_{max} \cdot \frac{[S1]}{KM1 \cdot (1+\frac{[P1]}{KP1}) + [S1](1+\frac{[S1]}{KS1})(1+\frac{[Gluc]}{K_{Iu1Gluc}})(1+\frac{[GDL]}{K_{Iu2GDL}})} \cdot \frac{[S2]}{KM2(1+\frac{[P2]}{KP2}) + [S2]}$$

The resulting parameters are summarized in Table 2.3.3-2 for *Lb*ADH and Table 2.3.3-3 for GDH. A residual plot of the predicted reaction rates versus the measured initial reaction rates indicates the quality of the estimated parameters and measurements (Figure 2.3.3-3).

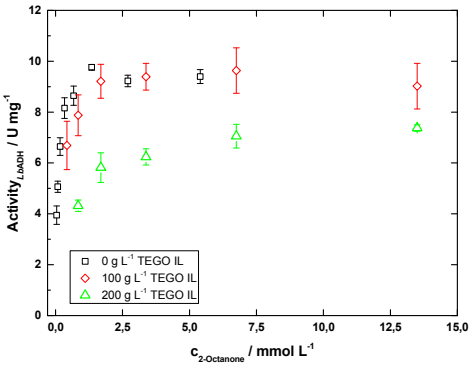

Figure 2.3.3-2: LbADH-activities for the 2-octanone-reduction at 0 g L^{-1} (squares), 100 g L^{-1} (diamonds), and 200 g L^{-1} (triangles) TEGO IL K5. $c_{ADA\text{-}buffer}$= 100 mmol L^{-1}, c_{MgCl2} = 10 mmol L^{-1}, pH=7.0, T = 25°C.

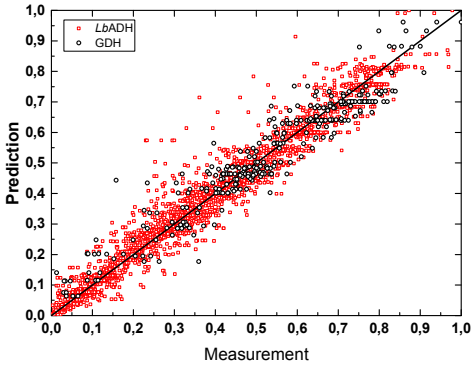

Figure 2.3.3-3: Normalised residual plot of all kinetic measurements, scaling with the maximum measured activity for LbADH and GDH separately; LbADH - squares (2626 data points); GDH - circles (319 data points); line - prediction = measurement.

c_{IL}, g L^{-1}	Parameter	Unit	2ON	2OL	2NN	2NL	2DN	2DL	3ON	3OL
0	*vmax*	U mg^{-1}	13.7 ± 0.77	7.8 ± 0.17	-	-	-	-	-	-
100	*vmax*	U mg^{-1}	17.3 ± 1.46	9.8 ± 1.28	17.7 ± 0.81	8.5 ± 0.73	17.3 ± 0.58	10.6 ± 0.63	12.7 ± 0.94	4.0 ± 0.85
200	*vmax*	U mg^{-1}	13.2 ± 1.07	8.0 ± 0.31	9.5 ± 0.68	6.1 ± 0.58	9.0 ± 0.94	6.4 ± 0.65	5.1 ± 0.17	2.3 ± 1.18
0	KM1	mmol L^{-1}	0.054 ± 0.008	0.115 ± 0.010	-	-	-	-	-	-
100	KM1	mmol L^{-1}	0.209 ± 0.045	0.847 ± 0.222	0.534 ± 0.061	1.438 ± 0.261	1.137 ± 0.082	3.937 ± 0.543	2.846 ± 0.491	3.154 ± 1.145
200	KM1	mmol L^{-1}	0.628 ± 0.139	1.292 ± 0.188	0.780 ± 0.192	4.253 ± 0.875	1.797 ± 0.499	8.778 ± 2.212	3.217 ± 0.523	17.083 ± 13.506
0	KM2	mmol L^{-1}	0.027 ± 0.003	0.013 ± 0.001	-	-	-	-	-	-
100	KM2	mmol L^{-1}	0.036 ± 0.007	0.034 ± 0.007	0.021 ± 0.002	0.014 ± 0.003	0.032 ± 0.003	0.027 ± 0.002	0.021 ± 0.005	0.015 ± 0.002
200	KM2	mmol L^{-1}	0.035 ± 0.006	0.018 ± 0.003	0.015 ± 0.003	0.014 ± 0.002	0.006 ± 0.001	0.006 ± 0.001	0.005 ± 0.001	0.004 ± 0.001
0	KP1	mmol L^{-1}	0.030 ± 0.005	0.055 ± 0.006	-	-	-	-	-	-
100	KP1	mmol L^{-1}	0.186 ± 0.060	0.501 ± 0.119	0.485 ± 0.073	0.361 ± 0.057	2.506± 0.462	0.971 ± 0.123	1.905± 0.463	6.129 ± 1.701
200	KP1	mmol L^{-1}	0.684 ± 0.201	0.119 ± 0.022	1.003 ± 0.362	0.576± 0.096	2.648 ± 1.067	1.596 ± 0.359	3.337 ± 1.158	4.642 ± 1.710
0	KP2	mmol L^{-1}	0.110 ± 0.017	0.008 ± 0.001	-	-	-	-	-	-
100	KP2	mmol L^{-1}	0.185 ± 0.040	0.013 ± 0.003	0.045 ± 0.005	0.014 ± 0.003	0.116 ± 0.010	0.011 ± 0.001	0.102 ± 0.102	0.024 ± 0.005
200	KP2	mmol L^{-1}	0.135 ± 0.024	0.027 ± 0.005	0.043 ± 0.010	0.007 ± 0.001	0.008± 0.002	0.005 ± 0.001	0.035 ± 0.012	0.009 ± 0.003
0	KluGluc	mmol L^{-1}	2985 ± 739	5992 ± 2268	-	-	-	-	-	-
100	KluGluc	mmol L^{-1}	≥1 E+4	4019 ± 2343	4522 ± 1181	5000 ± 3000	≥1 E+4	≥1 E+4	≥1 E+4	≥1 E+4
200	KluGluc	mmol L^{-1}	7517 ± 5107	≥1 E+4	2752 ± 1010	≥1 E+4	≥1 E+4	≥1 E+4	≥1 E+4	≥1 E+4
0	KluGDL	mmol L^{-1}	3818 ± 1563	≥1 E+4	-	-	-	-	-	-
100	KluGDL	mmol L^{-1}	1631 ± 430	391 ± 82	726 ± 78	667 ± 173	4321 ± 1413	≥1 E+4	≥1 E+4	≥1 E+4
200	KluGDL	mmol L^{-1}	1437 ± 378	1566 ± 477	1826 ± 668	≥1 E+4	1179 ± 584	2438 ± 1853	3255 ± 2484	≥1 E+4
0	KS1	mmol L^{-1}	560 ± 47	≥1 E+4	-	-	-	-	-	-
100	KS1	mmol L^{-1}	192 ± 55	192 ± 314	178 ± 38	119 ± 48	≥1 E+4	≥1 E+4	≥1 E+4	19 ± 11
200	KS1	mmol L^{-1}	287 ± 81	≥1 E+4	277 ± 94	153 ± 79	276 ± 285	≥1 E+4	≥1 E+4	76 ± 119

Table 2.3.3-2: Kinetic constants for *Lb*ADH measured with fluorescence spectrometry at 25°C for different substrates: 2-octanone (2ON), 2-octanol (2OL), 2-nonanone (2NN), 2-nonanol (2-NL), 2-decanone (2DN), 2-decanole (2DL), 3-octanone (3ON) and 3-octanol (3OL). Further conditions: c_{LbADH} = 1.25 mg L^{-1}, $c_{ADA\text{-}buffer}$ = 100 mmol L^{-1}, c_{MgCl2} = 10 mmol L^{-1}, $c_{TEGO\ IL\ 5K}$=0, 100, 200 g L^{-1}, pH = 7.

c_{IL}, g L^{-1}	Parameter	Unit	Value	Error
0	*vmax*	U mg^{-1}	5.4	0.24
100	*vmax*	U mg^{-1}	5.3	0.32
200	*vmax*	U mg^{-1}	3.1	0.15
0	KM1	mmol L^{-1}	6.756	1.274
100	KM1	mmol L^{-1}	1.931	0.336
200	KM1	mmol L^{-1}	1.313	0.312
0	KM2	mmol L^{-1}	0.027	0.002
100	KM2	mmol L^{-1}	0.026	0.004
200	KM2	mmol L^{-1}	0.017	0.003
0	KP1	mmol L^{-1}	> 1 E+4	
100	KP1	mmol L^{-1}	> 1 E+4	
200	KP1	mmol L^{-1}	> 1 E+4	
0	KP2	mmol L^{-1}	0.036	0.004
100	KP2	mmol L^{-1}	0.027	0.006
200	KP2	mmol L^{-1}	0.046	0.011
0	KS1	mmol L^{-1}	4210	1068
100	KS1	mmol L^{-1}	8366	3860
200	KS1	mmol L^{-1}	9128	4115

Table 2.3.3-3: Kinetic constants for GDH measured with with fluorescence spectrometry at 25°C. c_{GDH} = 5 mg L^{-1}, $c_{ADA\text{-}buffer}$ = 100 mmol L^{-1}, c_{MgCl2} = 10 mmol L^{-1}, $c_{TEGO\ IL\ 5K}$=0, 100, 200 g L^{-1}, pH = 7.

Substrate surplus inhibition and inhibition by glucose and GDL were included in the model used for parameter estimation. Due to numerical constraints, all constants were limited to 10 mol L^{-1}. Comparing the parameter sets for different experimental sets some trends are apparent. For example, v_{max} is strongly

depending on the position of the keto-group. This is especially the case for the main reaction M at an IL concentration of 100 g L^{-1}. In this case, v_{max} is the same within the error margin for the ketone reduction of 2-octanone, 2-nonanone, and 2-decanone. However, for the reduction of 3-octanone, v_{max} is substantially lower. Furthermore, the Michaelis-constant for the substrate, KM1 is strongly influenced by the presence of the IL. The higher the IL-content, the higher is KM1, the lower the enzyme's affinity for the substrate. Although, the apparent v_{max} for the LbADH-reaction indicates an activation at 100 g L^{-1} compared to 0 g L^{-1} and 200 g L^{-1} IL, the measured activities are nearly the same in 0 and 100 g L^{-1} and are only slightly reduced when using a buffer-solution containing 200 g L^{-1} (see Figure 2.3.3-3). Furthermore, inhibition is reduced so that at higher concentrations the rates are comparable. Initial rate experiments were also carried out with two different lots of GDH. It turned out, that both lots are covered by the same set for the kinetic constants.

2.3.4. Continuous enzymatic reduction of 2-octanone to *(R)*-2-octanol

Two main obstacles for the production of enantiopure long-chain alcohols with alcohol dehydrogenases are the low solubility of substrate and products in water and the low enzyme utilization. In this project a combination of techniques was used to overcome these limitations. The ionic liquid TEGO IL 5K was used as detergent to increase the low solubility for the starting materials and the products. The low enzyme utilisation was increased by using ultrafiltration in an enzyme membrane reactor (EMR). Both enzymes, alcohol dehydrogenase from Lactobacillus brevis (*Lb*ADH) and dehydrogenase from Bacillus sp. (GDH), were retained inside the reactor by a polyethersulfone membrane (ø= 63 mm, Sartorius) with a cut-off of 10,000 Da. Based on kinetic characterisation and stability data of *Lb*ADH and GDH, used for ketone reduction and cofactor regeneration, respectively, a continuous process with recycle of the aqueous phase was realized (Figure 2.3.4-1).

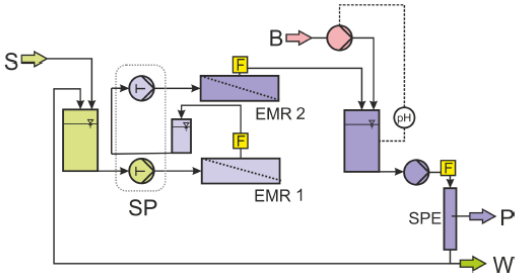

Figure 2.3.4-1: Flow scheme of the cascade of two EMR with integrated down-stream processing. S: Substrate solution, B: base, P: product by reextraction, W: 10% waste, EMR: enzyme membrane reactor, SP: syringe pump equipped with two pairs of syringes running synchronously, F: flow cells for automated sampling for gas chromatography, SPE: solid phase extraction/adsorption.

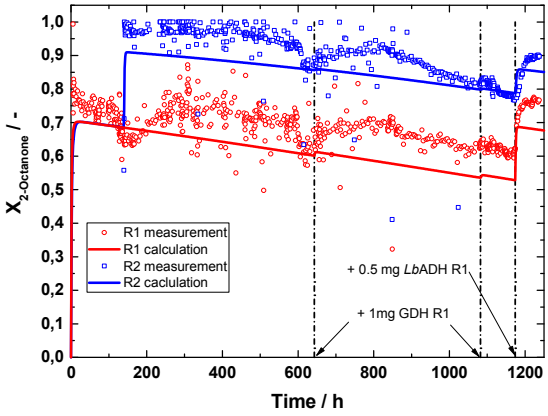

Figure 2.3.4-2: Conversion X as a function of time for continuous synthesis of *(R)*-2-octanol. Comparison of experiment (symbols) and model prediction (solid lines). Conditions: c^0_{LbADH} = 67 mg L^{-1} in each reactor, c^0_{GDH} = 280 mg L^{-1} in each reactor, added 1 mg GDH in R1 at 643 h and at 1083 h, added 0.5 mg LbADH in R1 at t = 1174 h. Further conditions: $c_{2\text{-octanone}}$ = 60 mmol L^{-1}, c_{NADP+} = 0.1 mmol L^{-1}, $c_{Glucose}$ = 200 mmol L^{-1}, c_{ADA} = 150 mmol L^{-1}, c_{MgCl2}=10 mmol L^{-1}, $c_{TEGO\ IL}$ = 100 g L^{-1}, dV/dt = 4 ml h^{-1}, pH = 7.0, T = 25°C.

A configuration of a cascade of two enzyme membrane reactors (each with V = 15 mL) was chosen, which allows information to be gained and use to be made of the high reaction rate in the first reactor (conversion of 76%, Figure 2.3.4-2). After 140 h of stable operation, a second reactor was added, leading to nearly full conversion in the outlet of the second reactor (Figure 2.3.4-2). Both substrate and product were analyzed via GC (FID). Down-stream processing (DSP) was done via solid phase extraction (SPE) in a stainless steel column filled with HR-P material (Macherey-Nagel, Germany). At its outlet the 2-ketone and 2-alcohol content was determined via GC as well. If less than 0.5 mmol L^{-1} was detected, the solution was reused for synthesis. In order to avoid accumulation of GDL and depletion of glucose in the system, 10% of the solution was replaced by a fresh solution of the ketone, glucose and the cofactor $NADP^+$, after adjusting the pH to the initial value. In order to compensate for the degraded enzyme, 1 mg GDH was dosed into the first reactor after 643 and 1083 h runtime and 0.5 mg *Lb*ADH were added at a runtime of 1174 h (Figure 2.3.4-2). Both times, dosing GDH led to a slight increase in conversion. However, the highest improvement

was achieved dosing supplemental *Lb*ADH into the reactor. A continuous dosage of the enzyme was not used as the overall stability of the reaction system was of interest. In total, a stable operation for 1250 h was possible. Until the dosage of LbADH at 1174 h a turnover number TON_{LbADH} of 4.6×10^7 and TON_{GDH} of 7.7×10^6 were reached for the first reactor. Further key parameters of the reaction are summarised in Table 2.3.4-1. The data of the kinetic experiments (Chapter 2.3.3) were used to predict the conversion in this setup, assuming a half-life of 1000 h for both enzymes. The results are also shown in Figure 2.3.4-2 (solid lines). The overall trend and the enzyme dosage steps are well represented and reflected in the model as well.

Time, h	R	X[a]	TON[b]$_{LbADH}$	TON[b]$_{GDH}$	TON[c]$_{NADP+}$	STY[a]/ mmol L^{-1} d^{-1} (/ g L^{-1} d^{-1})	ee	E-Factor[a,(d)]
1174	1	75.8	4.6×10^7	7.7×10^6	411	291 (37.9)		
1250	2	96.9	1.3×10^7	2.9×10^6	539	124 (16.1)	>= 99.9	132 (13.2)

Table 2.3.4-1: Key parameters for the continuous enzymatic reduction of 2-octanone to *(R)*-2-octanol. X – conversion, R – reactor, [a] after 24 h runtime, [b] at the end of reaction, [c] per pass through the reactor, [d] with recycling.

2.3.5. Cofactor monitoring under reaction conditions

2.3.5.1. Batch experiments

In order to significantly increase solubility of the substrate for the monophasic approach of the enzymatic 2-octanone reduction, the ionic liquid TEGO IL 5K was added to the reaction mixture. Unfortunately, this IL possesses a high fluorescence signal itself (Figure 2.3.5-1). Therefore, in order to implement cofactor monitoring via FS spectrometry in this case the background signal of the matrix should always be taken into consideration.

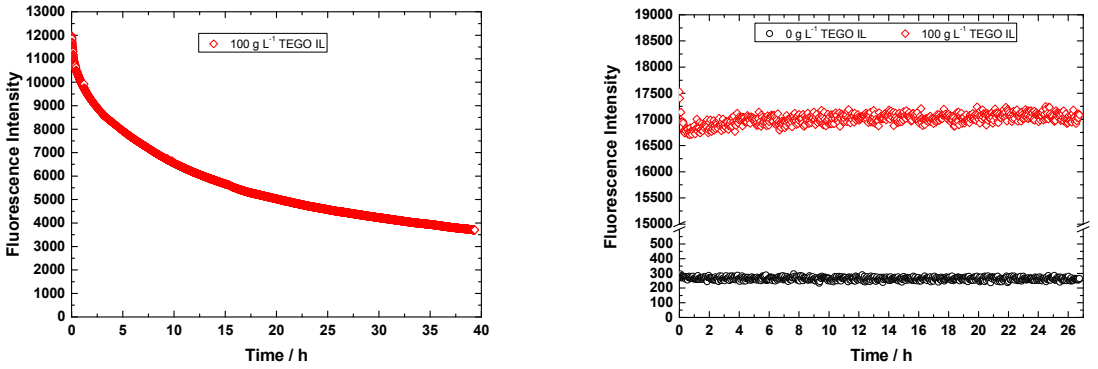

Figure 2.3.5-1: Fluorescence signal of the ionic liquid TEGO IL 5K measured with the FS-probe (left) and UV/VIS multiplate fluorescence reader (right), $c_{ADA\text{-}buffer}$= 100 mmol L^{-1}, c_{MgCl2} = 20 mmol L^{-1}, T = 25°C.

Nevertheless, several batch experiments in presence of the ionic liquid were performed with integrated cofactor monitoring. First measurements were performed inside the fluorescence multi plate reader Synergy MX allowing online monitoring of the NADPH concentration up to 10 hours. Conversion of 2-octanone was measured by GC (FID). Figure 2.3.5-2 summarises measurements and model predictions for different start concentrations of $NADP^+$ (100, 75, 50 and 10 µM). It is apparent that with decreasing $NADP^+$ start concentration model prediction and actually measured NADPH concentration via multiplate reader fit better. For 100, 75 and 50 µM $NADP^+$ the predicted NADPH concentration is consistently 2 to 3 times higher than measured. And even for the best correlation for 10 µM $NADP^+$, the model still cannot describe accurately the beginning of the reaction. However, the model fits the measured 2-octanone conversion rather good, especially for the critical start region. Slight deviations are observed for the lowest $NADP^+$ start concentration.

Further on, batch experiments were performed in a separate reactor set-up with approx. 30 ml volume. Here, NADPH concentrations were followed via the FS-probe. 2-octanone conversion was measured via GC (FID). The obtained results for different $NADP^+$ start concentrations are represented in Figure 2.3.5-3 with the respective model predictions. Again the model exhibits difficulties in describing measured NADPH concentration, especially for the start region. But still for the range of complete 2-octanone conversion model and measurement for NADPH come closer. And again the model was able to describe the measured 2-octanone conversion.

In all cases up to here the start range for the NADPH concentration was largely overestimated by the model, when starting the reaction with $NADP^+$. A possible explanation might be, that the measured NADPH

concentration in the reaction solution is not the actual one at the active catalytic sites, as NADPH might be generated by GDH and directly *"in situ"* consumed by *Lb*ADH in a shorter time period as needed for diffusion into the solution. In order to exclude such effects, several experiments were performed with NADPH present at the beginning of the reaction. Figure 2.3.5-4 summarises experimental results and model prediction for 100 and 50 µM NADPH initial concentration in combination of FS-probe measurement.

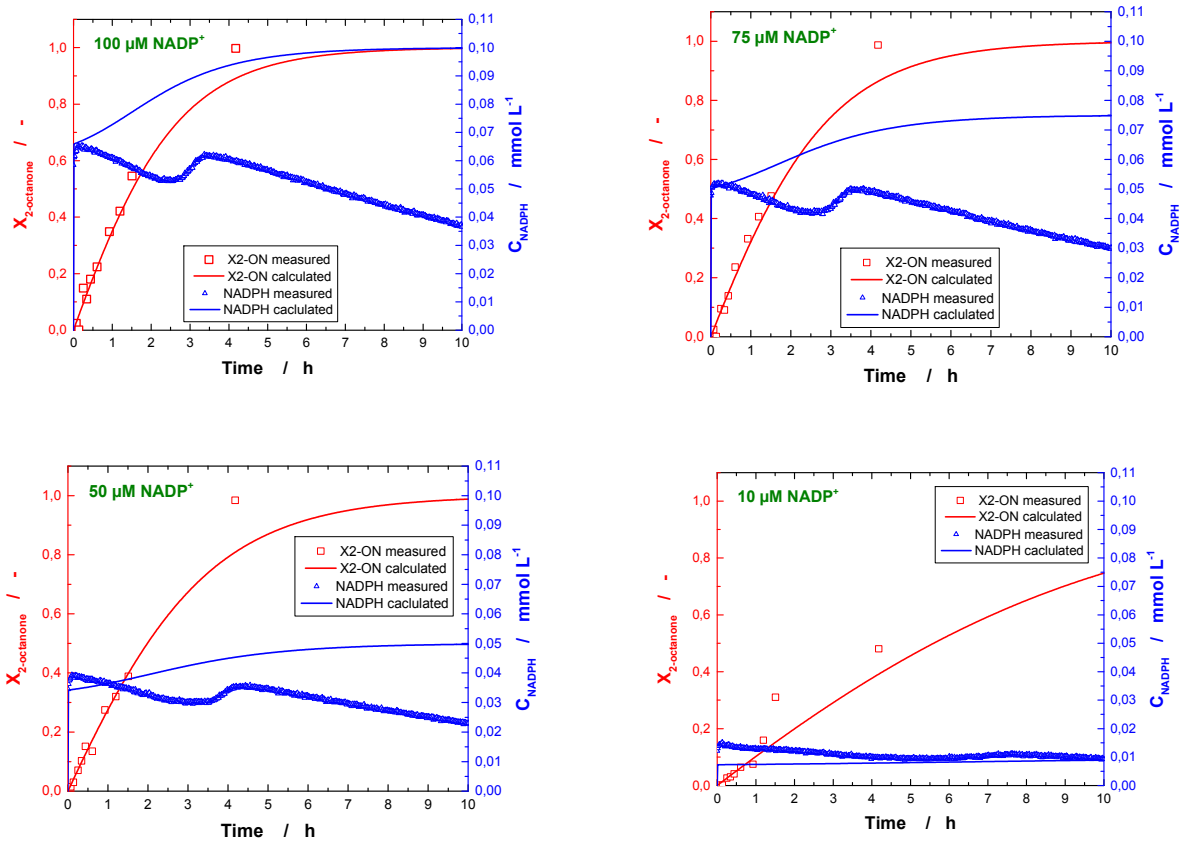

Figure 2.3.5-2: Batch experiments with combination of fluorescence multiplate reader (C_{NADPH}, mmol L^{-1}) and GC measurement ($X_{2\text{-}ON}$) with 100 g L^{-1} IL at different start $NADP^+$ concentrations. Comparison of experimental data and model prediction. Further conditions: C_{ADA} = 150 mmol L^{-1}, C_{MgCl2}=20 mmol L^{-1}, $c_{2\text{-Octanone}}$ = 60 mmol L^{-1}, $c_{Glucose}$ = 200 mmol L^{-1}, c_{LbADH} = 50 mg L^{-1}, c_{GDH} = 250 mg L^{-1}, T = 25°C.

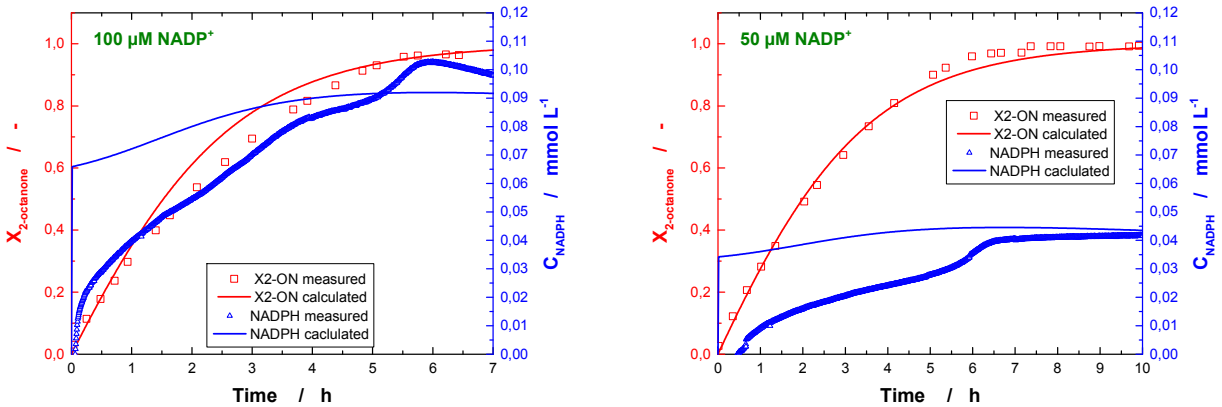

Figure 2.3.5-3: Batch experiments with combination of FS-probe measurement (C_{NADPH} mmol L^{-1}) and GC measurement ($X_{2\text{-}ON}$) with 100 g L^{-1} IL at different $NADP^+$ start concentrations. Comparison of experimental data and model prediction. Further conditions: C_{ADA} = 150 mmol L^{-1}, C_{MgCl2}=20 mmol L^{-1}, $c_{2\text{-Octanone}}$ = 60 mmol L^{-1}, $c_{Glucose}$ = 200 mmol L^{-1}, c_{LbADH} = 50 mg L^{-1}, c_{GDH} = 250 mg L^{-1}, T = 25°C.

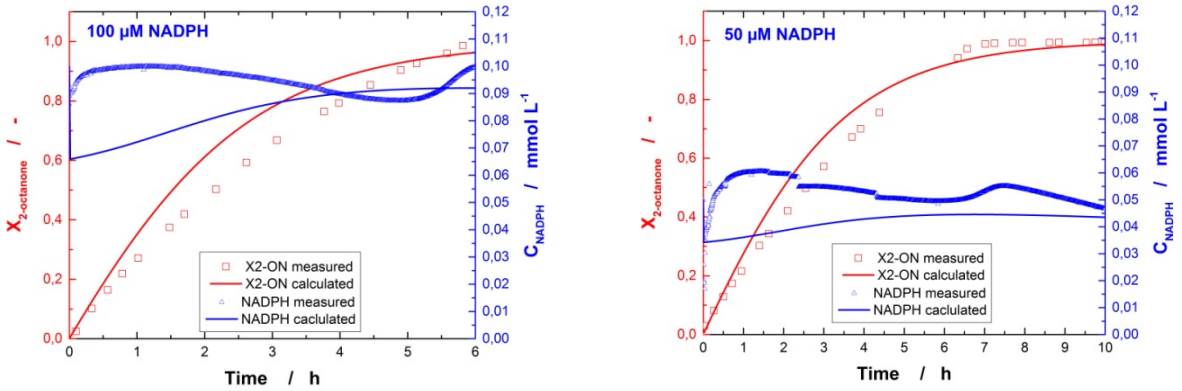

Figure 2.3.5-4: Batch experiments with combination of FS-probe measurement (C_{NADPH} mmol L^{-1}) and GC measurement ($X_{2\text{-}ON}$) with 100 g L^{-1} IL at different NADPH start concentrations. Comparison of experimental data and model prediction. Further conditions: C_{ADA} = 150 mmol L^{-1}, C_{MgCl2}=20 mmol L^{-1}, $c_{2\text{-}Octanone}$ = 60 mmol L^{-1}, $c_{Glucose}$ = 200 mmol L^{-1}, c_{LbADH} = 50 mg L^{-1}, c_{GDH} = 250 mg L^{-1}, T = 25°C.

Here the opposite effect is observed: the measured NADPH concentration is consistently higher than the predicted one. This behaviour might as well indicate diffusion limitations due to which NADPH is "accumulated" in the solution and much slowly consumed as calculated by the model, which do not account for such effects.

2.3.5.2. Continuous experiments

For the continuous enzymatic reduction of 2-octanone to *(R)*-2-octanole, first online measurements of cofactor concentrations were performed in the set-up represented in Figure 2.3.5-5. Here the ionic liquid TEGO IL 5K was not used as solubiliser in order to avoid correction for its fluorescence effects. Therefore, only a very low substrate concentration (6 mmol L^{-1} 2-octanone) in the aqueous phase was possible and as a result no separate pH adjustment of the recycled solution was required. The FS-probe was mounted in a flow cell (ca. 30 mL) at the enzyme membrane reactor outlet after the flow cell for the online GC measurement (V= 150 µL) of the 2-octanone and 2-octanol concentrations. A recycle of the aqueous phase was implemented as described in Chapter 2.3.4. The FS-probe was operated at 5% intensity of the LED unit, in order to avoid degradation effects due to the constant sample irradiation (Figure 2.3.2-2). The results of a continuous reaction run up to 800 h are represented in Figure 2.3.5-6.

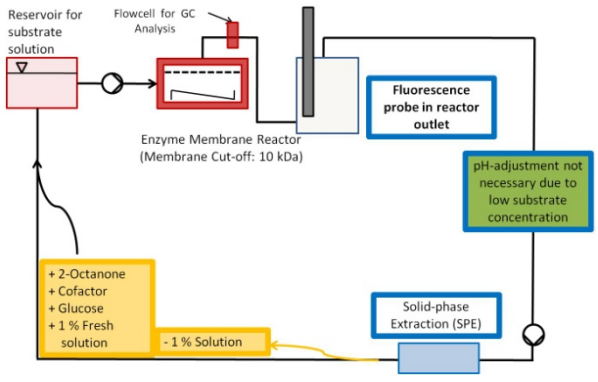

Figure 2.3.5-5: Experimental set-up for continuous enzymatic 2-octanone reduction with online measurement of NADPH concentrations and recycle of the aqueous phase.

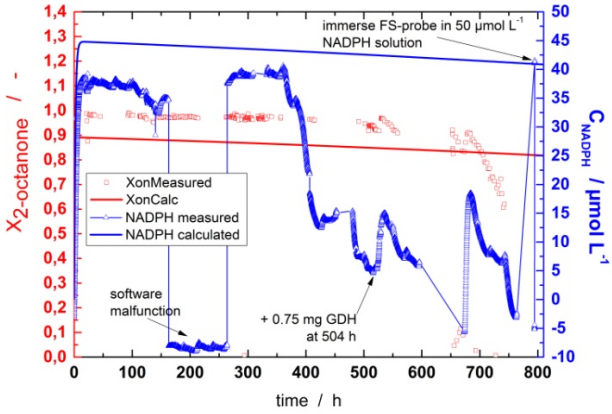

Figure 2.3.5-6: 2-octanone conversion (left axis) and NADPH concentration (right axis) for a continuous process with the set-up in Figure 2.3.5-5. Reaction conditions: $c_{2\text{-}octanone}$ = 6 mmol L^{-1}, c_{LbADH} = 50 mg L^{-1} (0.75 mg), c_{GDH} = 100 mg L^{-1} (1.5 mg), c_{NADP^+} = 0.05 mmol L^{-1}, $c_{glucose}$ = 100 mmol L^{-1}, $c_{ADA\text{-}buffer}$= 100 mmol L^{-1}, c_{MgCl2} = 10 mmol L^{-1}, T = 25°C, pH = 7, dV/dt = 8 ml h^{-1}, τ = 1.5 h.

The conditions for the experiment in Figure 2.3.5-6 were chosen optimal for the 2-octanone conversion. And indeed very stable performance of the system was observed until 500 hours runtime with conversion greater than 95%. From 500 h to 680 h a slight decrease of conversion was observed (ca. 90%) with a sudden decrease afterwards (ca. 60%). Interestingly, a drop in the NADPH concentration at ca. 370 h was observed (almost a factor of 3), which apparently did not affect *Lb*ADH productivity until 500 h runtime. Moreover, the addition of fresh GDH at 504 h did slightly increased NADPH concentration but it did not reach its maximal value. However, the immersion of the FS-probe in 50 µM NADPH solution lead to an increased signal, verifying that this analytical tool apparently functioned as expected.

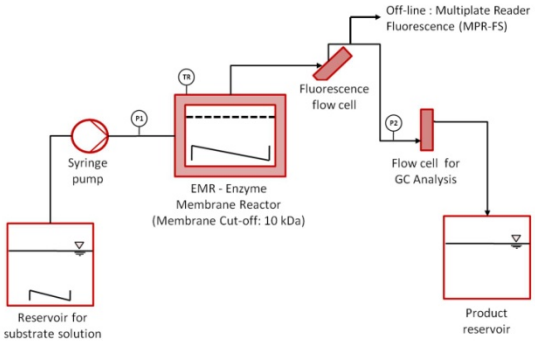

Figure 2.3.5-7: Simplified reaction set-up for continuous 2-octanone reduction without recycle of the aqueous phase.

The experiment represented in Figure 2.3.5-6 demonstrated the feasibility of the cofactor monitoring via FS for continuous processes but left many open questions regarding its accuracy and the reasons for the observed fluctuations. Therefore, for the last project phase a second continuous set-up without the recycle of the aqueous phase was realised (Figure 2.3.5-7). Experimental results are summarised in Figure 2.3.5-8.

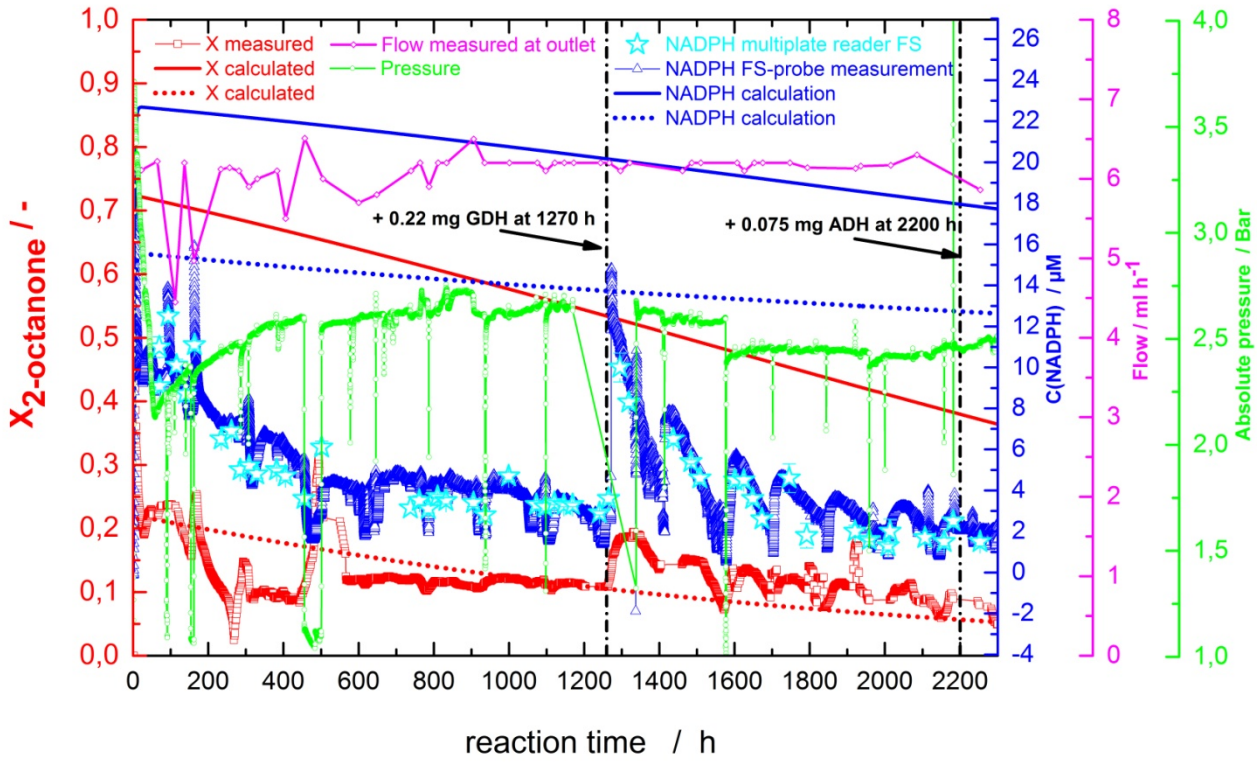

Figure 2.3.5-8: Conversion of 2-octanone (left axis), as well as NADPH concentration (right axis 1), volume flow (right axis 2) and absolute pressure (right axis 3) for a continuous process with the set-up in Figure 2.3.5-7. Reaction conditions: $c_{2\text{-octanone}}$ = 2 mmol L^{-1}, c_{LbADH} = 10 mg L^{-1}(0.15 mg), c_{GDH} = 30 mg L^{-1}(0.45 mg), c_{NADP^+} = 0.025 mmol L^{-1}, $c_{glucose}$ = 100 mmol L^{-1}, $c_{ADA\text{-}buffer}$= 100 mmol L^{-1}, c_{MgCl2} = 10 mmol L^{-1}, T = 25°C, pH = 7, dV/dt = 6 ml h^{-1}, τ = 2.5 h. Solid line – model prediction calculated with the experimental conditions. Dotted line – model prediction assuming membrane leak calculated with one tenth of the enzymes concentrations.

The new set up was simplified with the focus on the online cofactor detection. Therefore, a new flow cell for the FS-probe was constructed with the smallest possible volume of 3.6 ml and the shortest possible mean residence time respectively, where the probe was mount in 45° angle (optimal according to manufacturer to avoid gas bubbles accumulation). With the help of an on/off valve directly at the flow-cell outlet, samples of ca. 0.5 ml were withdrawn and analyzed off-line for the NADPH concentration with the UV/VIS multiplate fluorescence reader. The FS-probe flow cell was connected directly at the EMR reactor outlet with the shortest possible tubing, before the flow cell for GC analysis. Due to the implementation of a shutter, the LED source was modulated so that 100% lamp intensity was used with 5 minutes sampling interval (120 ms irradiation). A pressure sensor was mounted before the membrane in order to detect possible membrane fowling or leakage. The system flow was verified at least once a day at the product reservoir. Substrate 2-octanone and product 2-octanol were detected via GC (FID). Enantiomeric excess (*ee*) of the product was not determined as the previous experiments have all shown a stable very high *ee*. Reaction conditions were deliberately chosen to avoid total 2-octanone conversion, in order to be able to directly see how the changes in cofactor concentration affect the system. Compared to the previous experiment (Figure 2.3.5-6) ADH and GDH concentrations were reduced from 50 and 100 mg L^{-1} to 10 and 30 mg L^{-1}, respectively, $NADP^+$ concentration was reduced from 50 to 25 µmol L^{-1} and substrate concentration was reduced from 6 to 2 mmol L^{-1} 2-octanone. All other conditions were kept the same.
With this set-up the continuous process was run for almost 100 days (2300 h), Figure 2.3.5-8. As no recycle of the medium was implemented, the substrate solution reservoir (1L) had to be changed every 150 h run time (at maximum), which is indicated by the regular pressure drops, when the pump was stopped to change the bottles (Figure 2.3.5-8). The pressure drop between 455 h and 497 h was due to malfunction of the pump. And the lack of pressure signal between 1169 h and 1339 h was due to malfunction of the data acquisition software of the pressure sensor.
The results represented in Figure 2.3.5-8 and Figure 2.3.5-9 suggest that the membrane itself plays the most important role in the system. Its properties seem to be changing in the first 500 hours run time, indicated by the drastic changes of pressure (especially for the first 60 hours) as well as the fluctuation of the system flow and the 2-octanone conversion. Looking more closely at the data at the beginning of the experiment (Figure 2.3.5-9) we see that within the first hour the pressure drops completely and then rises quickly to an even higher value than at start. This behaviour might indicate an initial membrane leak that is later closed due to swelling effects, which would lead to leaching of the enzymes and therefore reduce the effective concentration of both enzymes inside the EMR.

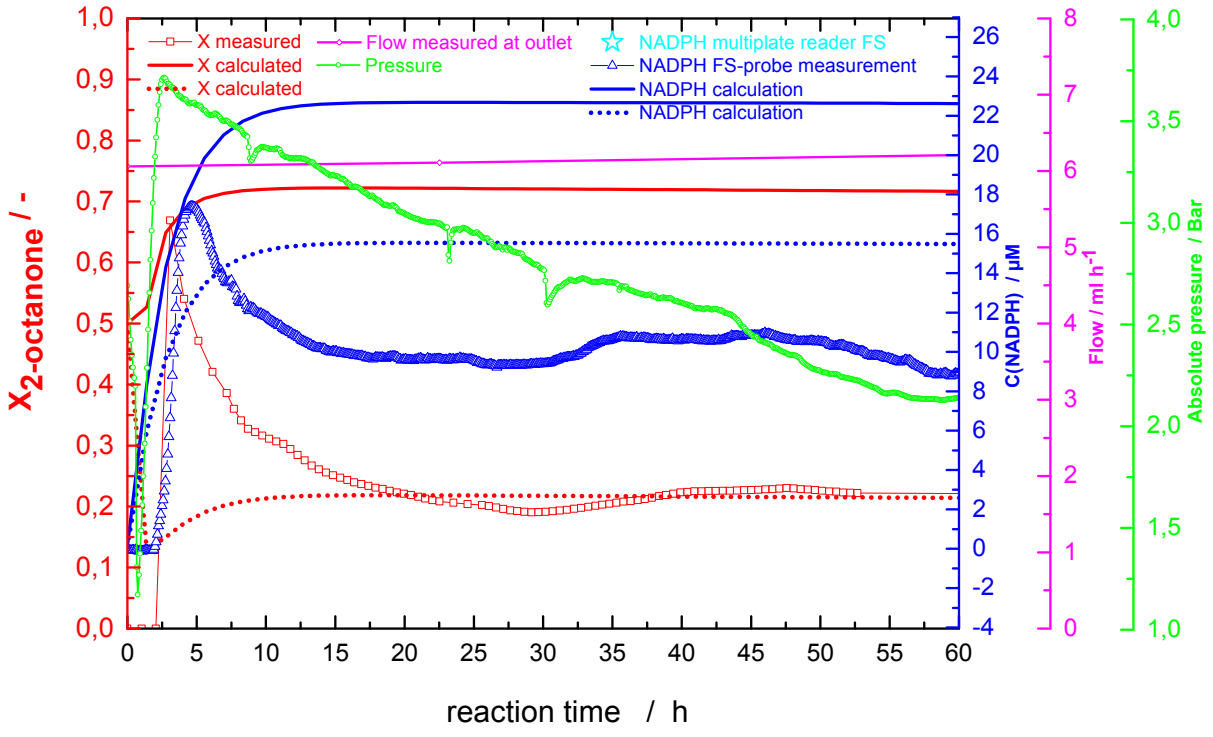

Figure 2.3.5-9: The first 60 hours of the experiment represented in Figure 2.3.5-8.

It is obvious that pressure changes in reactor are directly connected to changes in the NADPH signal (Figure 2.3.5-8). Generally, the FS-probe delivers the “true” concentration in the system, confirmed by the offline measurements with the fluorescence multiplate reader. After an initial loss of GDH activity (or a decrease of GDH concentration due to a membrane leach), indicated by a drop in the NADPH signal especially during the first 200 h and then up to 500 h, a stable performance is observed afterwards. The addition of fresh GDH in the system at 1270 h run time (Figure 2.3.5-8) increased the NADPH signal almost to the initial value, however, a rather fast drop (ca. 200 h compared to ca 500 h at the beginning of the experiment) to the previous level was observed. And from this point on, a faster drop of NADPH concentration in between the changes of the reaction solution reservoir is observed as well. The reasons for the latter are not clear at the moment. The addition of fresh *Lb*ADH at 2200 h did not bring a measurable effect in the NADPH signal.
Regarding the convergence between mathematical model prediction and measurement we see that in this case the discrepancies are significant. Whereas for the reaction represented in Figure 2.3.5-6 model and measurement fit better together (at least before the NADPH signal drop) here deviations larger than 50% are observed (Figure 2.3.5-8 straight lines). A possible membrane leak leading to overestimated enzyme concentrations inside the reactor could explain this, as the calculation with ten times lower enzymes concentrations (Figure 2.3.5-8 dotted lines) lead to a much better fit of 2-octanone conversion. However, real NADPH concentration remains rather overestimated by the model, similar to the observations for the batch experiments (Chapter 2.3.5.1).
The key parameters for the experiment in Figure 2.3.5-8 are summarized in Table 2.3.5-1. We see, that despite the deliberately unfavourable conditions for the reaction, thanks to the extremely stable system and long runtime remarkably high turn over numbers (TON) for *Lb*ADH and GDH are observed, comparable to the results for the optimised continuous process with recycle of the aqueous phase (Table 2.3.4-1).

Time, h	X^a	TON^b_{LbADH}	TON^b_{GDH}	TON^c_{NADP+}	STY^a/ mmol L^{-1} d^{-1} (/ g L^{-1} d^{-1})
2343	23.8	1.3×10^7	$1.4\ 10^6$	18	4.3 (0.56)

Table 2.3.5-1: Key parameters for the continuous enzymatic reduction of 2-octanone to *(R)*-2-octanol in Figure 2.3.5-8. X – conversion, R – reactor, [a] after 100 h runtime, [b] at the end of reaction, [c] per pass through the reactor.

2.4. Stellungnahme, ob Ergebnisse der Vorhaben wirtschaftlich verwertbar sind

Die Ergebnisse zeigen klar, dass es eine Differenz zwischen der modellbasierten Vorhersage und den tatsächlichen NADPH-Konzentrationen unter Prozessbedingungen gibt. Daher sind in-situ Messungen sehr wichtig, um effiziente Bioprozesse mit den entsprechenden Enzymen zu betreiben. Das inline Monitoring erlaubt die präzise Nachdosierung der einzelnen Systemkomponenten, um den Prozess ständig im optimalen Prozessfenster zu halten, ohne unwirtschaftlich hohe Enzym- oder Cofaktormengen zu verwenden. Die hier erzielten Ergebnisse haben daher direkte Relevanz für die Wirtschaftlichkeit von Bioprozessen und könnten in der Entwicklung von entsprechenden kommerziellen inline-Monitoringsystemen resultieren.

2.5. Wer hat zu den Ergebnissen des Projekts beigetragen

Prof. Dr. Lasse Greiner und Prof. Dr. Jens Schrader als Projektleiter.
Projektbearbeiter: Dr. Susanne Leuchs, Susanne Bohl, Dr. Jonathan Bloh, Dr. Aneta Pashkova

2.6. Qualifikation des wissenschaftlichen Nachwuchses

Im Zusammenhang mit dem Projekt wurden folgende Qualifikationen erreicht:
Promotion: Dr. Susanne Leuchs
Bachelorarbeit Susanne Bohl

2.7. Literaturverzeichnis

[1] N. Kimura, T. Fukuwatarıl, R. Sasaki, K. Shibata, J. Nutr. Sci. Vitaminol., 52/2 (2006) 142–148, doi: 10.3177/jnsv. 52.142.
[2] M. Eckstein, T. Daussmann, U. Kragl, Biocatal. Biotransform., 2/22 (2004) 89–96, doi: 10.1080/10242420410001692769
[3] J. T. Wu, L. H. Wu, J. A. Knight, Clin. Chem, 32 (1986) 314-319

3. Zusammenfassung (Summary)

Nicotine amide dinucleotide cofactors are of paramount importance for the industrial utilisation of the enzyme class of oxidoreductases. For their rational use a knowledge gap exists between predictions based on initial rate measurements and their application in processes. The main goal of the project is the online quantification of cofactors under process conditions by application of fluorescence spectrometry allowing monitoring of the reduced form of the cofactors at µmol L^{-1} which are common in their application.
Two techniques were established for quantitative NADPH detection: microplate fluorescence measurement and fiber optical fluorescence measurement. Both were validated in the range of 1 to 100 µmol L^{-1} NADPH. Stable calibration factors were obtained for routine use under process conditions.
As a model reaction the enzymatic reduction of 2-octanone to (*R*)-2-octanol via alcohol dehydrogenase from Lactobacillus brevis (*Lb*ADH) was thoroughly investigated. A monophasic approach was developed with the addition of a ionic liquid to the aqueous buffer phase serving as solubiliser and allowing to work at much higher substrate concentrations. An enzyme coupled cofactor regeneration with glucose dehydrogenase from *Bacillus spec* (GDH) and glucose as hydride donor (cosubstrate) was used for better utilization of the cofactor ($NADP^+$/NADPH). Beside routine batch experiments, a continuous process was realised. In a configuration of a cascade of two enzyme membrane reactors the process could be demonstrated for more than 1000 hours with *Lb*ADH turnover numbers of more than 4×10^7 and space-time yield of up to 34 g L^{-1} d^{-1} with 99.9% enantioselectivity. Furthermore, downstream processing via adsorption of the alcohols was included, allowing 90% recycle of the aqueous buffer. Thus, the E-factor (amount of waste stream per product) was reduced to 13. For both batch and continuous synthesis a mathematical model with Michaelis-Menten type kinetics has been developed and implemented for process optimisation.
As quantitative data about cofactor concentrations under process conditions is unavailable, major part of the work was the cofactor stability measurements for the model enzymatic process. For this, NADPH was identified as the most critical and was focused on. The measurements validate findings from literature, for example deteriorative influence of phosphate, (acetate), elevated temperatures, UV-radiation, and H^+-ions. Whereas, Mg^{2+} -ions, low temperatures, OH^--ions, and the ionic liquid TEGO IL K5 do increase half-life. Unprecedented, higher stability of NADPH at higher initial NADPH concentrations was observed. In general, the complexity of our findings, in combination with data derived from literature, support our recommendation to measure cofactor stabilities for the conditions which will be applied in the intended process as quantitative literature data is sparse and possibly not applicable.
Fulfilling the main goal of the project, online monitoring of cofactor concentrations has been demonstrated for the model reaction in batch and continuous mode. Comparison with model predictions as well as with offline measurements has been used as a tool for process optimisation. In batch mode experiments were performed with both multiplate reader and FS-probe detection of NADPH. In all cases reaction times of up to 10 hours were achieved. In this case the implemented mathematical model was able to describe the substrate conversion rather well, whereas deviations between predicted and measured NADPH concentrations were observed, especially for the start of the reaction, presumably due to diffusion effects. For the continuous experiments we demonstrated an application with integrated NADPH monitoring via the FS-probe in a simplified set-up for reaction times of over 3 months. Via offline measurements with the multiplate fluorescence reader, it was confirmed that the fiber optical FS-probe delivers the “true” cofactor concentration. Again the conversion coincided well with the model prediction while the NADPH concentration in the reactor deviated strongly from the prediction, underlining the importance of in-situ measurements. Further on, the membrane inside the enzyme membrane reactor set-up plays an important role in the process. Directly connected with it pressure changes or leaks affect the cofactor concentration immediately. Enzyme stability and productivity is the other major factor.
In summary we may say that online NADPH monitoring via FS spectroscopy is possible and it brings further insight into the enzymatic process investigated. It is a useful tool which can be implemented to optimize the process in real time and compensate for diverse effects of pressure or enzyme loss, e.g., by membrane leaching. A limitation is the condition that the substrate and further components of the reaction mixture should not be fluorescent species, as a correction factor should be implemented, which might not be experimentally accessible in each case. Degradation effects due to light source intensity should be taken into consideration as well. Nevertheless, we think that the findings as a result of our work are essential for the rational usage of cofactors in reductive in vitro biotransformations.